Hybridization of Lunar Mantle Sources by Garnet-Bearing Cumulates During Overturn Reconciles the REE, and Nd and Hf Isotopic Characteristics of High-Ti Basalts. J. L. Scholpp and N. Dygert, Department of Earth and Planetary Sciences, University of Tennessee, Knoxville (jscholpp@vol.utk.edu)

Introduction: Ilmenite-bearing cumulates (IBC) are thought to precipitate from a lunar magma ocean (LMO) after ~90%-98% solidification [1, 2]. IBC contain silicates (Cpx and plagioclase) and Fe-Ti oxides (e.g., ulvöspinel and ilmenite), giving them high density with respect to underlying cumulates. This gravitationally unstable density stratification promotes formation of downwelling Rayleigh-Taylor instabilities that sink into the underlying lunar mantle, a process known as cumulate overturn [3, 4]. Previous studies hypothesize that mixing of overturned IBC with deep LMO cumulates forms hybridized mantle sources capable of producing high-Ti basalts [5-7]. Petrogenetic models indicate that garnet (Grt) might be involved in the petrogenesis of some lunar glasses and basalts owing to their HREE depletion [8, 9]. Numerical simulations [13], high-pressure experiments on proposed lunar mantle sources [11], and new experiments investigating phase equilibria relevant to overturned IBC and interactions between downwelling IBC and ambient lunar mantle (Scholpp and Dygert, 2023, this meeting) [12] show that Grt is stable in downwelling IBC at pressures >2GPa, and mantle sources hybridized by IBC may be Grt-bearing. To investigate the role of Grt in IBC on lunar mantle hybridization and mantle melting, we model the REE and isotopic compositions of cumulates of a solidifying LMO assuming an LPUM bulk composition [13]. LMO cumulate compositions are then used to model the formation of hybridized Grt-free and Grt-bearing mantle sources. Partial melting of the hybridized Grt-free and Grt-bearing lherzolite (LHZ) sources is then modeled and compared to natural samples. The REE and isotopic compositions of high-Ti glasses and basalts are most successfully modeled by partial melting of a Grt-bearing LHZ hybridized by melts of overturned Grt-bearing IBC.

LMO Solidification Model: The REE, Lu-Hf isotope, and Sm-Nd isotopic compositions of the LMO cumulates were modeled based on the crystallization sequence and mineral proportions of [2]. This model assumes fractional crystallization occurs throughout the sequence of LMO solidification, and 1% trapped interstitial liquid is incorporated into LMO cumulates. The bulk REE and isotopic composition of the LMO is assumed to be chondritic [14, 15]. As a simplification, we assume that no radioactive decay occurs during the duration of LMO solidification (i.e., LMO solidification is effectively instantaneous), and the LMO has an isotopic composition equivalent to CHUR [15] at 4.4 Ga. The Lu-Hf and Sm-Nd systems evolve according to fractionation of elemental ratios of Lu/Hf and Sm/Nd after initial chondritic ratios. Modeled LMO cumulates have higher Yb/Sm than glasses and basalts (Fig. 1a) and higher $^{176}Lu/^{177}Hf$ ratios than basalts (Fig. 1b). LMO residual liquids overlap with glass REE compositions (Fig. 1a), but the residual liquids do not to overlap with the isotopic compositions of basalts (Fig. 1b).

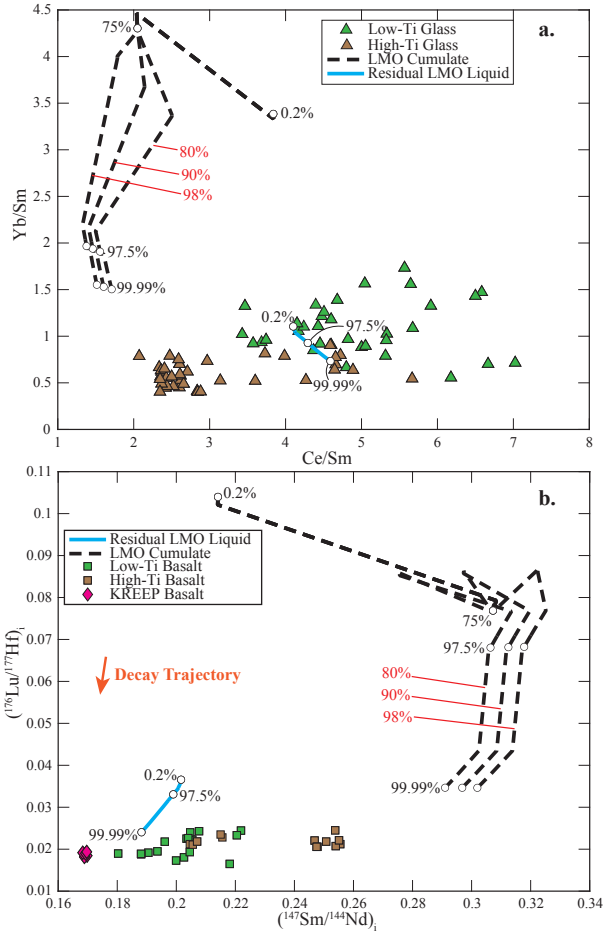

Fig. 1. Evolution of residual LMO liquid and cumulates during fractional crystallization of the LMO compared to REE abundances in lunar glasses (a), and (b) isotopic compositions of lunar basalts. (a) Symbol for low-Ti glass represents low and very low-Ti glass groups; symbol for high-Ti glasses represents yellow, orange, red, and black glass groups. Glasses are compiled from [16]; basalt isotope data are compiled from [6, 17, 18]. Basalt isotope ratios are age corrected to initial ratios. Percentages in black represent the extent of LMO crystallization. Percentages in red represent different plagioclase floatation efficiencies. Orange arrow in (b) represents the approximate trajectory of isotopic evolution as decay occurs over time.

Hybridization and Partial Melting Model: Following the results of our experiments [12], hybridization is assumed to occur between melts of overturned IBCs and lunar mantle dunite, producing Grt-free and Grt-bearing LHZ sources. The REE and isotopic composition of a cumulate that formed at 98.6% LMO solidification is

assumed to represent the IBC. A mean early cumulate composition that forms between 1% and 51% LMO solidification is used for the dunite. Aggregated partial melts from 20% melting of the IBC hybridize the dunite. Grt-free IBC melting assumes the non-modal melting reaction from [5] [Eq (1)]; Grt-bearing IBC melting uses a modified version of Eq (1) [Eq (2)].

Eq (1). 63 Cpx + 37 Ilm = 100 Melt

Eq (2). 52 Cpx + 37 Ilm + 11 Grt = 100 Melt

For the Grt-bearing IBC, we assume that the modal abundance of Grt is equal that of plagioclase from the solidification model (1.4-12.7% depending on floatation efficiency). Hybridization of the lunar mantle assumes that assimilation and mechanical mixing generate a source that is ~80% dunite and ~20% IBC melt. After calculating the compositions of these hybridized sources, we model their partial melting and compare the model predictions to lunar basalts and glasses. We assume non-modal melting and use published melting reactions for Grt-free [19] and Grt-bearing [20] LHZ. For Grt-free sources, models assume melting continues until Cpx is exhausted (i.e., F≈19%). For Grt-bearing sources models assume melting continues beyond Grt exhaustion (F≈7%).

Results: Hybridized sources only exhibit HREE and Lu-Hf isotope depletion comparable to lunar basalts if Grt was present in the downwelling, hybridizing IBC, forming Grt-bearing sources (Fig. 2, red stars). Melts of Grt-free sources hybridized by melts of Grt-free IBC reproduce the REE trends of some low-Ti and high-Ti glasses (Fig. 2a, gray dashed lines); however, these melts cannot account for any lunar basalt isotopic compositions (Fig. 2b). Partial melting of Grt-bearing sources hybridized by melts of Grt-bearing IBC reproduces the REE abundances of most high-Ti lunar glasses (Fig. 2a, red dash-dotted lines) and reproduces the isotopic compositions of most lunar basalts (Fig. 2b). Most high-Ti glasses and basalts fall between the trends for models with 90% and 98% plagioclase floatation efficiency in REE and isotope space.

Implications: Our models demonstrate the important role of Grt in the petrogenesis of the lunar basalts. While [10, 21] found that Grt could be a LMO cumulate for a Moon with an aluminous TWM (Taylor Whole Moon) composition, a TWM bulk composition would produce excessive plagioclase modes inconsistent with the thickness of the lunar crust [2, 22]. In contrast, overturned IBC have sufficient Al_2O_3 concentrations to stabilize Grt in overturned IBC at pressures >2GPa [12], even if the bulk LMO had a low-Al LPUM-like composition. Our models imply that hybridization between, Grt-bearing IBC and early LMO cumulates, forming Grt-bearing hybridized sources account for the HREE depleted signatures and isotopic compositions of many high-Ti glasses and basalts. In the context of crustal constraints on lunar bulk composition, basalts and glasses with heavy REE depletion may be strong evidence of partial melting of hybridized sources in the Grt stability field at pressures >2GPa, and delivery of Grt to those hybridized sources by downwelling of IBCs during cumulate mantle overturn events.

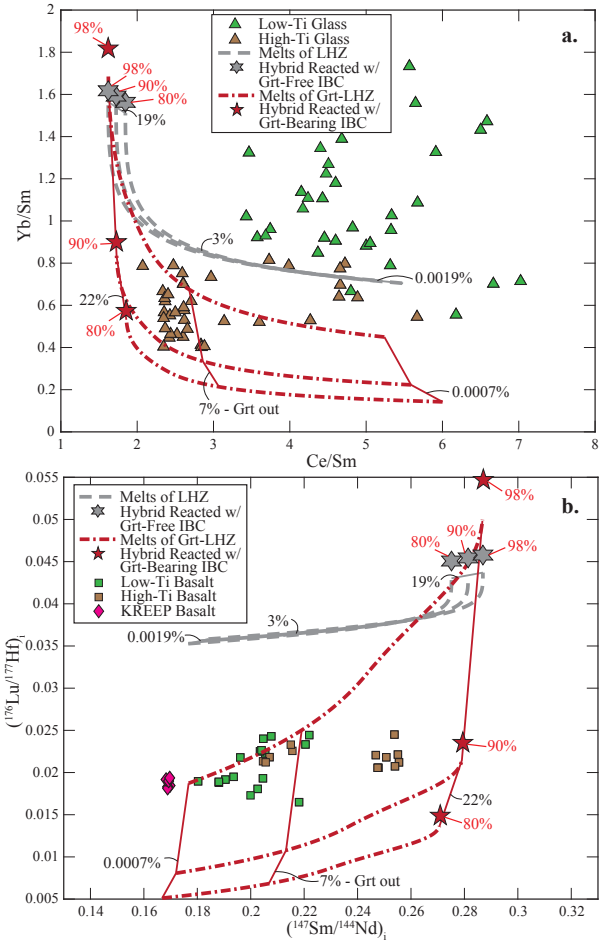

Fig. 2. Hybridized lunar mantle melting with Grt-free and Grt bearing LHZ sources. Colors of melting trends match colors of their source symbols. Black values = percent melting, Red values = a model's assumed plagioclase floatation efficiency.

References: [1] Elkins-Tanton et al. (2011), *EPSL*, *304*, 326-336. [2] Charlier et al. (2018), *GCA, 234*, 50-69. [3] Hess & Parmentier (1995), *EPSL*, *134*, 501-514. [4] Zhang et al. (2017), *GRL*, *44*, 6543-6552. [5] Van Orman & Grove (2000), *MPS*, *35*, 783-794. [6] Sprung et al. (2013), *EPSL*, *380*, 77-87. [7] Brown & Grove (2015), *GCA, 171*, 201-215. [8] Snyder et al. (1992), *GCA, 56*, 3809-3823. [9] Neal (2001), *JGR, 106*, 865-885. [10] Johnson et al. (2021), *EPSL*, *556*, 116-721. [11] Mallik et al. (2019), *GCA, 250*, 238-250. [12] Scholpp & Dygert (2023), *LPSC LIII*, Abstract Submitted. [13] Longhi (2006), *GCA, 70*, 5919-5934. [14] Anders & Grevesse (1989), *GCA, 53*, 197-214. [15] Bouvier et al. (2008), *EPSL*, *273*, 48-57. [16] Shearer & Papike (1993), *GCA, 57*, 4785-4812. [17] Unruh et al. (1984), *JGR, 89*, 459-477. [18] Beard et al. (1998), *GCA, 62*, 525-544. [19] Kinzler & Grove (1992), *JGR, 97*, 6885-6906. [20] Walter (1998), *JP, 39*, 29-60. [21] Elardo et al. (2011), *GCA, 75*, 3024-3045. [22] Taylor & Wieczorek (2014), *Phil. Trans. R. Soc.*, *372*.